

Interaction of the Depolarization-Activated K⁺ Channel of *Samanea saman* with Inorganic Ions: A Patch-Clamp Study^{1, 2}

Nava Moran*, David Fox, and Ruth L. Satter

Department of Neurobiology, Weizmann Institute of Science, Rehovot 76100 Israel (N.M.); Jefferson Alumni Hall, Thomas Jefferson Medical College Philadelphia, Pennsylvania 19107 (D.F.); and Department of Molecular and Cell Biology, University of Connecticut, Storrs, Connecticut 06268 (R.L.S.)

ABSTRACT

A depolarization-activated K⁺ channel capable of carrying the large K⁺ currents that flow from shrinking cells during movements of *Samanea saman* leaflets has been described in the plasma-lemma of *Samanea* motor cell protoplasts (N Moran *et al* [1988] *Plant Physiol* 88:643–648). We now characterize this channel in greater detail. It is selective for K⁺ over other monovalent ions, with the following order of relative permeability: K⁺ > Rb⁺ > Na⁺ ≈ Cs⁺ ≈ Li⁺. It is blocked by Cs⁺ and by Ba²⁺ in a voltage dependent manner, exhibiting a 'long-pore' behavior, similarly to various types of K⁺ channels in animal systems. Cadmium, known for its blockage of Ca²⁺ channels in animal systems, and Gd³⁺, closely related to La³⁺, which also blocks Ca²⁺ channels in animal cells, both block K⁺ currents in *Samanea* in a voltage-independent manner, and without interfering with the kinetics of the currents. The suggested mechanism of block is either (a) by a direct interaction with the K⁺ channel, but external to its lumen, or, alternatively, (b) by blocking putative Ca²⁺ channels, and preventing the influx of Ca²⁺, on which the activation of the K⁺ channels may be dependent.

Leaflet movements in *Samanea saman* and other nyctinastic legumes depend upon changes in the volume of motor cells in the pulvini. Motor cell volume changes are driven osmotically, by changes in the concentration of internal K⁺, Cl⁻, and other solutes (reviewed in ref. 24). Cells in the extensor region of the pulvinus take up K⁺ and Cl⁻ as they swell during leaflet opening, and lose both ions as they shrink during leaflet closure, while cells in the opposing (flexor) region behave in the reverse manner. In 1981, Satter and Galston (22) postulated a role for ionic channels in the transport of ions across *Samanea* motor cell membranes.

We recently (17, 18, 23, 24) described a potassium channel in plasma membranes of protoplasts isolated from the extensor or flexor region of the *Samanea* pulvinus. Our data suggest

that this channel plays a role in the passive efflux of K⁺ during cell shrinkage. The channel has the following characteristics: (a) it is voltage gated, opening upon membrane depolarization with a time constant of 1 to 2 s; (b) at moderate depolarizations, it does not inactivate for many minutes; (c) its conductance ranges from 15 to 40 pS at external K⁺ concentrations between 5 and 125 mM, respectively; (d) it can be blocked by TEA³ and quinine, compounds that block K⁺ channels in membranes of other organisms; and (e) the channel is similar in both extensor and flexor cells.

TEA and quinine also inhibited the movement of excised leaflets, thereby supporting the view that the flow of K⁺ current through these channels is necessary for leaflet movement. To characterize this channel in greater detail, we now extend our description of the channel's 'signature' to include its interaction with various inorganic ions: Li⁺, Na⁺, Rb⁺, Cs⁺, Ba²⁺, Cd²⁺, and Ga³⁺. Preliminary results appeared in abstract form (18).

MATERIALS AND METHODS

Plant Material

Samanea saman trees were grown in a greenhouse, as described by Moran *et al.* (17). Terminal secondary pulvini were excised from the third and fourth mature leaves, counting from the apex, within 3 h after dawn.

Protoplast Isolation

Protoplasts were isolated separately from the extensor and flexor regions of the pulvinus using the method for protoplast isolation described by Moran *et al.* (17), or a modification of this method. Our modification was as follows. After 30 to 35 min of enzymatic digestion, the tissue was separated from the enzyme solution by filtration on a double layer of 50 μm nylon mesh. The enzyme solution was discarded, and the tissue was rinsed off the mesh into a B5-Gamborg's solution (basic composition as in GIBCO catalog [1985, Netherlands], and containing in addition 100 mM KCl, 340 mM sorbitol, 2 mM CaCl₂, 0.5 mM DTT) and was agitated occasionally for 10 min. This tissue and cell suspension was then layered on

¹ This manuscript is dedicated to Ruth L. Satter.

² Supported by United States-Israel Binational Science Foundation, Jerusalem, Israel, grant 87-00278 to N.M.; Basic Research Foundation, the Israel Academy of Sciences and Humanities grant 487/89 to N.M.; Binational U.S.-Israel Agricultural Research and Development grant US-963-85 to N.M. and R.L.S., and C. Mischke; and U.S. National Science Foundation grant DMB 83-04613 to R.L.S.

³ Abbreviations: TEA, tetraethylammonium; BAPTA, 1,2-bis(o-aminophenoxy)ethane-N,N',N',N'-tetraacetic acid.

a Ficoll cushion and spun at approximately 360g for 7 min, resulting in a green layer just above the Ficoll cushion. The clear solution on top of the green layer was discarded. Cold B5-Gamborg's solution (containing in addition 240 mM sorbitol, 240 mM sucrose, 30 mM KCl, 2 mM CaCl_2 , and 0.5 mM DTT) was then layered on top of the green band, and the gradient was spun at 64g for 5 min. Protoplasts were collected from an uppermost 4 to 5 mm layer and kept on ice for up to 20 h. We used flexor cells for most experiments described here; extensor cells were used where noted in figure captions.

Recording Solutions for Patch-Clamp Experiments

The bath solution contained varying concentrations of K^+ and/or other ions (Rb^+ , Cs^+ , Ba^{2+} , etc.), 1 mM CaCl_2 , 10 mM Mes at pH 5.8 to 6.0, and about 0.45 to 0.55 M sorbitol (used to adjust the final osmolarity of the solution to 550 to 580 mOsm). The internal (pipette) solution contained 10 to 20 mM Hepes at pH 7.1 to 7.2, 14 to 215 mM KCl with or without a test ion, and either Ca/EGTA buffer (6) or Ca/BAPTA (Sigma) buffer to yield a free Ca^{2+} concentration between 4×10^{-8} and 3×10^{-6} M, 1 to 2.5 mM MgATP (Sigma), and about 0.4 M sorbitol, to adjust the final osmolarity of the solutions to 600 to 620 mOsm.

Temperature

The experiments were conducted at room temperature of 23 to 26°C, but temperature did not vary more than 1°C during a single experiment.

Patch-Clamp Experiments

The patch-clamp technique is described in detail by Hamill *et al.* (11); application of the patch-clamp methodology to plant cells is described by Satter and Moran (23), and Moran *et al.* (17). Briefly, a drop of the protoplast suspension was added to 1.5 mL of the recording solution and the protoplasts were allowed to settle and stick to the bottom of the experimental chamber, a Nunc (Roskilde, Denmark) tissue culture dish. The patch pipette was then brought into contact with the protoplast. Upon the formation of a tight seal between the patch electrode and the cell membrane, the patch was broken to form a 'whole-cell' configuration. At this configuration, the solution within the pipette becomes continuous with the cytoplasm, and within several seconds to a few minutes replaces the diffusible components of the cytoplasm.

All experiments were performed in a voltage-clamp mode using the Axopatch B-1 amplifier (Axon Instruments, Burlingame, CA) and were under computer control (an IBM clone, Minta AT, Taiwan) using a software-hardware system from Axon Instruments (pclamp program package software and the TL1-TM-100 Labmaster A/D and D/A peripherals).

Membrane potential was varied according to a pre-programmed schedule and the resulting membrane current was filtered at 20 Hz (-3 db), digitized at 100 Hz, and stored for further analysis. The error in voltage clamping of the whole-cell membrane, largely due to the access resistance of the patch pipette, was compensated at 80% by analog circuitry of the Axopatch amplifier.

Electrophysiology: Determination of Reversal Potential and Relative Permeability

Two pulse sequences were used in these experiments:

1. To monitor the voltage and time dependence of K^+ channels, a series of increasingly depolarizing, single square pulses, each lasting 15 to 30 s (e.g. Fig. 1A), was applied at intervals of 20 mV and 30 to 45 s (between start of pulses). The holding potential was restored between pulses. These pulses would usually activate outward currents, followed, upon the restoration of the holding potential, by deactivating tail-currents.

2. To calculate the relative permeability of different ions (as outlined below), the reversal potential had to be determined, by a series of paired pulses, applied at 30 to 45 s intervals. This constitutes the 'tail-current' method, for the determination of reversal potential (illustrated in Fig. 1, C and D). The membrane potential was stepped to a certain depolarized value (pre-pulse) to open K^+ channels, and then to another potential (test-pulse), to elicit a (deactivating) tail-current. At the end of the test pulse, the holding potential was restored. Several pairs of pulses (pre-pulse/test-pulse) were repeated: the pre-pulse was always the same for a given series, while the test-pulse ranged from -90 to -10 mV (usually aimed at the vicinity of the presumed reversal potential; Fig. 1C). A plot of the instantaneous tail-currents (corrected for leakage current, as described by Moran *et al.* [17]) as a function of the potential at which they were recorded (the values of the test-pulses) yields the instantaneous I-V curve (Fig. 1D). This, in turn, yields the reversal potential, *i.e.* the zero-current potential, or the potential at which no current flows, although the channels are open. If the solutions bathing the membrane contain only a single permeant ion, the reversal potential equals the ion's Nernst potential; when two or more permeant ions are included, the reversal potential reflects a combination of their Nernst potentials, weighted by their

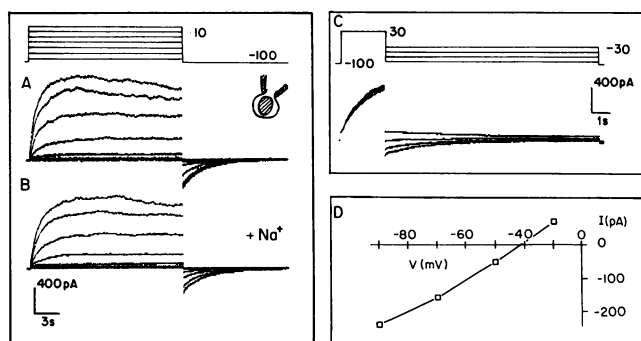


Figure 1. The effect of external Na^+ on K^+ currents. Whole-cell membrane currents (superimposed "noisy" traces) elicited by a series of square voltage pulses (also superimposed, *top panel*). Holding potential was -100 mV. (A) Control; *inset*: recording configuration. (B) After addition of 25 mM Na^+ to the external solution. C and D, A 'tail-current' experiment for the determination of reversal potential. The experimental solutions contained: bath: 6 mM K^+ , 550 mM sorbitol, 1 mM CaCl_2 , 10 mM Mes (pH 6.0); pipette: 139 mM K^+ , 125 mM Cl^- , 450 mM sorbitol, 2 mM MgATP, 2 mM BAPTA- Na_4 , 0.5 mM CaCl_2 (calculated free Ca^{2+} concentration was 40 nM), and 20 mM Hepes (pH 7.2).

relative permeabilities. Thus, the permeability of a permeating cation X^+ , relative to that of K^+ (P_X/P_K), can be calculated from the reversal potential, E_{rev} , using the Goldman equation (7):

$$(1) \quad E_{rev} = -\frac{RT}{F} \ln \frac{[K^+]_i + P_{Cl^-}/P_K [Cl^-]_o + P_X/P_K [X^+]_i}{[K^+]_o + P_{Cl^-}/P_K [Cl^-]_i + P_X/P_K [X^+]_o}$$

with P_{Cl^-}/P_K and P_X/P_K denoting the permeabilities of Cl^- and the cation X^+ , respectively, relative to that of K^+ (we assumed the relative permeability of an ion at the internal mouth of the channel to equal that at the external mouth). $[]_i$ and $[]_o$ denote the internal (pipette) and outer (bath) ion concentrations. R , T , and F are the universal gas constant, absolute temperature and Faraday constant, respectively. The anion used in our experiments was Cl^- , and in all calculations we used the value of 0.05 for the permeability ratio of Cl^- to that of K^+ (determined for 12 cells), unless it could be determined independently for the same cell. Note, that although Na^+ (8 mM) was present in most internal solutions with BAPTA, we disregarded this in our calculations for two reasons: (a) the control K^+ currents recorded in these conditions were comparable in their amplitudes and time courses to those recorded with internal EGTA, without Na^+ , and (b) the contribution of this to the error in calculation of P_X was less than 5%. The measured potentials were corrected for liquid-junction potentials resulting from different ion mobilities (21).

RESULTS

Na^+ and Li^+

Figure 1A depicts membrane currents elicited by a series of depolarizing square pulses. As previously demonstrated using similar experimental conditions (17), these currents are carried by K^+ ions via the depolarization-activated K^+ channel (K_D channel).

The addition of 25 mM of Na^+ (Fig. 1B) or of Li^+ (data not shown) to the external solution only slightly diminished both the outward and the inward membrane currents. Moreover, K^+ currents, in both directions, persist even in the presence of 50 mM external Na^+ (not shown).

To estimate the relative permeabilities of Na^+ and Li^+ in the K_D channel, we used the 'tail-current' method for the determination of the reversal potential for the currents (see "Materials and Methods"). This is illustrated for Na^+ in Figure 1, C and D. The calculated permeability for Na^+ , relative to that of K^+ , was 0.10 in this experiment, and 0.07 ± 0.05 on average (mean \pm SD; $n = 6$). The calculated relative permeability for Li^+ (data not shown) was 0.05 ± 0.02 ($n = 3$).

Rb^+

To determine the relative permeability of Rb^+ , we replaced most of the K^+ in the internal solution by Rb^+ . The outward currents recorded in these conditions (Fig. 2A) were within the range of voltage dependence and time constants of activation and deactivation of K^+ currents observed in similar conditions (with equivalent concentration of K^+ only inside), such as depicted in Figure 1. Thus, the gating properties of the channels conducting these currents were similar to those

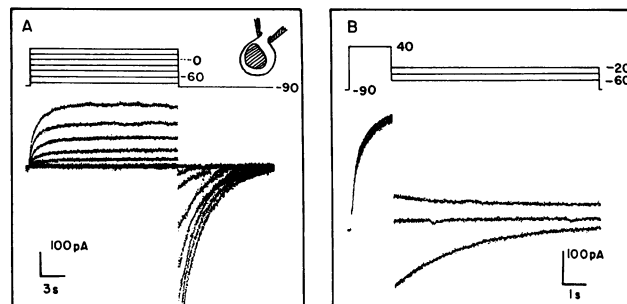


Figure 2. The permeability of Rb^+ in the K^+ channel. (A) Whole cell membrane currents (superimposed, bottom) elicited by a series of square voltage pulses (superimposed, top). The holding potential was -90 mV. Inset: the recording configuration. (B) A tail-current experiment, for the determination of the reversal potential. Solutions were as in Figure 1A, except for the following: bath: 16 mM K^+ , 12 mM Cl^- ; pipette: 14 mM K^+ , 125 mM Rb^+ .

of K_D channels. In addition, and similarly to K^+ currents, these currents could be abolished by 10 mM TEA (not shown). We therefore conclude that they were carried via the K_D channel. Since the prevalent cation in the internal (pipette) solution was Rb^+ (see legend) and in the external solution $-K^+$, we assume that the major ion carrier of the outward current was Rb^+ and that of the inward tail-current was K^+ .

Since the amplitude of the Rb^+ currents was somewhat smaller than the usual range of those observed for K^+ currents, the permeability of Rb^+ within the K_D channels must be somewhat smaller than that of K^+ . For more exact estimation of the relative permeability of Rb^+ , we used the tail-current method (illustrated in Fig. 2B). From the value of the reversal potential (-40 mV in this experiment), we estimate the permeability of Rb^+ in the K_D channel to be 0.75 that of K^+ . The average relative permeability of Rb^+ was 0.64 ± 0.24 ($n = 3$).

Cs^+

In Figure 3A most of internal K^+ was replaced by Cs^+ . Note both the virtual absence of outward currents and the presence of large inward tail currents elicited by restoring the holding potential after a depolarizing pulse. This is summarized in two current-voltage ($I-V$) curves in Figure 3B: the steady-state $I-V$ curve for the outward currents and the instantaneous $I-V$ curve for the tail-currents. The increasing amplitude of the instantaneous tail current, following the increasingly more depolarizing pulses, reflects the increase of membrane conductance during the depolarization, which was otherwise obscured due to the absence of the outward current. Figure 3C illustrates a tail-current experiment summarized in an instantaneous $I-V$ curve in Figure 3D. Since the tail-currents vanished in the presence of TEA (Fig. 3C), and since the prevalent cation in the external solution was K^+ (Fig. 3, legend), we conclude that the tail-currents were carried by K^+ via the K_D channel. The value of the reversal potential of the TEA-sensitive current was 3 mV, and the calculated permeability of Cs^+ in this experiment, relative to K^+ , was 0.06. The average relative permeability of Cs^+ was 0.05 ± 0.02 ($n = 3$).

The addition of Cs^+ at the external surface of the cell

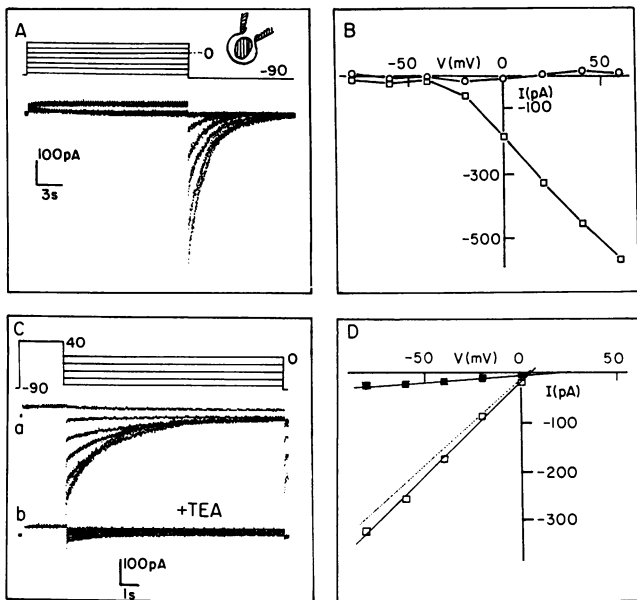


Figure 3. Effect of internal Cs^+ on K^+ current. (A) Current records (superimposed, bottom), elicited by a series of square voltage pulses (superimposed, top). The holding potential was -100 mV. (B) Current-voltage (I - V) relationships: steady-state (end-of-the-pulse) I - V curve (\circ); instantaneous I - V relationship for the tail currents recorded upon the return to the holding potential (\square). Abscissa: membrane potential during the pulse. (C and D) Tail-current method for determination of the reversal potential; tail currents before (\square) and after (\blacksquare) the addition of 10 mM TEA to the bath. Note the disappearance of these currents upon TEA treatment. Continuous lines: fitted by eye to the data points. Interrupted line: net, TEA sensitive tail current. Solutions as in Figure 1A, except bath: 20 mM K^+ , 16 mM Cl^- ; pipette: 14 mM K^+ , 125 mM Cs^+ .

membrane only partially diminishes outward K^+ currents. In contrast, inward tail-currents were abolished completely (Fig. 4B).

Ba^{2+}

Figure 5 depicts the complex effect of Ba^{2+} on the K^+ current, in the presence of 32 mM of external K^+ . Figure 5A shows the records of membrane currents elicited by repeating the same series of voltage pulses in the presence of varying external concentrations of Ba^{2+} . In Figure 5B, the peak values of these currents are plotted versus membrane potential during the depolarizing pulses. Barium (0.5 mM) decreased the outward current elicited by a depolarization to 30 mV by about 15 to 20% (Fig. 5B). In contrast, at -10 mV, as much as about half of the outward current was suppressed by 0.5 mM Ba^{2+} . In Figure 5C the instantaneous tail-currents at -100 mV (holding potential) are plotted versus the membrane potential preceding the tail-current. Note that 0.5 mM of external Ba^{2+} effectively blocked about 80% of the inward tail-current at -100 mV following a 30 mV depolarization, although it caused only about 20% block during the depolarization itself.

Figure 5D shows the effect of Ba^{2+} on the kinetics of channel gating. This is summarized in a plot of $t_{1/2}$ (the time to attain

half of the maximum value of the current, measured from the start of the voltage step) versus membrane potential during the voltage step. Here, too, the effect of Ba^{2+} was voltage dependent: Addition of 0.5 mM Ba^{2+} to the external solution roughly doubled the $t_{1/2}$ at 30 mV (from 0.6 s to 1.2 s), while it more than tripled $t_{1/2}$ at -10 mV (from 1.4 s to 4.8 s).

Figure 6 shows the effect of 1 mM Ba^{2+} on membrane currents in the presence of 7 mM external K^+ . In these conditions, over 80% of the outward current was suppressed at 30 mV, and the suppression was complete at -30 mV and more hyperpolarized potentials (Fig. 6B). The effect of Ba^{2+} was (at least partially) reversible (Fig. 6, A and B).

Note that while 1 mM external Ba^{2+} blocked about 80% of the outward current in the presence of 7 mM KCl (Fig. 6, at $+30$ mV), the same amount of Ba^{2+} suppressed only about 20% of the outward current when the external K^+ concentration was 32 mM (Fig. 5, at $+30$ mV).

Cd^{2+}

Figure 7 shows the effect of Cd^{2+} on K^+ currents. Cadmium (330 μM) blocked most of both outward and inward current. Figure 7A illustrates the reversibility of the Cd^{2+} block. Cadmium block was not voltage dependent: 330 μM Cd^{2+} , in the presence of 50 mM external K^+ , blocked about 90% of the current at $+40$ mV, and about 95% at -90 mV (tail-current at the holding potential).

Blockage of the K^+ current increased with the increase in Cd^{2+} concentration. This is summarized in Figure 7B, in a family of steady-state I - V curves, and in a dose-response curve (at membrane potential of 50 mV) in Figure 7C. The concentration for blockage of one-half the control current is about 60 μM Cd^{2+} . The dose-response curve at -10 mV practically overlaps (not shown).

In Figure 7D, current records are compared, before (left) and after (right) the addition of 80 μM Cd^{2+} to the external solution, in the presence of 7 mM K^+ . Although 80 μM Cd^{2+}

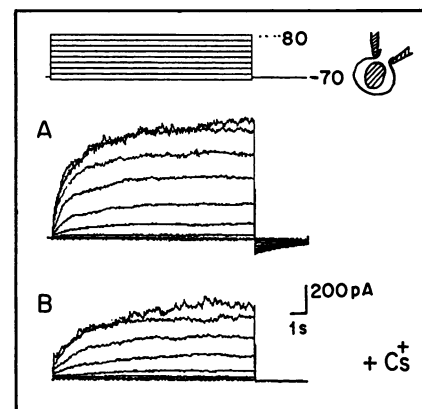


Figure 4. Effects of external Cs^+ and Na^+ . Membrane current recorded in response to a series of square voltage pulses (top). Before (A) and after (B) after the addition of 25 mM Cs^+ to external solution. The holding potential was -70 mV. Solutions: as in Figure 1A, except bath: 50 mM Na^+ , 10 mM K^+ , 56 mM Cl^- ; pipette: 125 mM KCl , 2 mM EGTA (instead of BAPTA), 0.6 mM Ca^{2+} (calculated free Ca^{2+} concentration was 0.5 μM [6]).

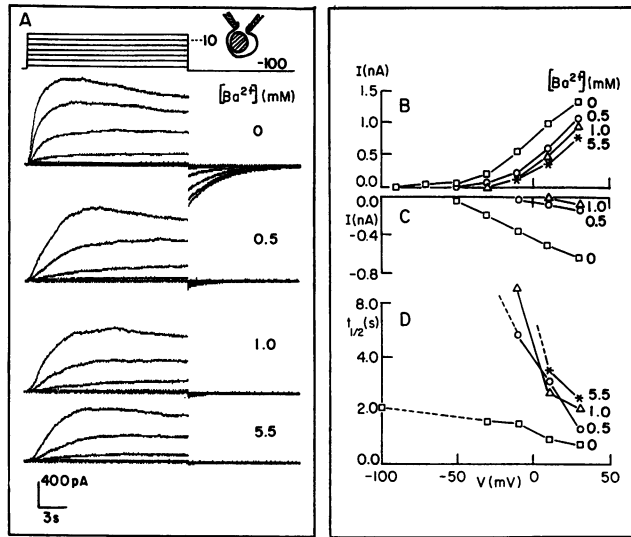


Figure 5. Effect of external Ba^{2+} . (A) Membrane currents (superimposed), in response to a series of square voltage pulses (also superimposed). The series was repeated at various external Ba^{2+} concentrations, indicated on each panel. (B) Peak-of-current I - V curves, with Ba^{2+} concentrations indicated to the right. (C) Instantaneous I - V curves of the tail-currents obtained upon the restoration of the holding potential. D: voltage dependence of $t_{1/2}$, i.e. the time to half-maximum current, measured from the start of the voltage step. Solutions: as in Figure 1A, except bath: 32 mM K^+ .

blocked about two-thirds of the K^+ current, the kinetics of the remaining current seems to be unaffected.

Gd^{3+}

The effect of Gd^{3+} is depicted in Figure 8. When a Gd^{3+} -containing pipette (200 μM Gd^{3+} in external solution) was positioned in the vicinity of the cell (30–50 μm away), membrane currents decreased by about 50% (Fig. 8C). Note, that similarly to Cd^{2+} and in contrast to Ba^{2+} , Gd^{3+} did not affect the time course of the remaining currents. The removal of the pipette resulted in restoration of the current amplitude (not shown). Figure 8A displays a family of I - V curves, at various concentrations of Gd^{3+} (denoted to the right). Figure 8B summarizes the concentration-dependence of Gd^{3+} blockage. The concentration for blockage of one-half the current was about 17 μM .

DISCUSSION

In an attempt to characterize the depolarization-activated K_D channel in the plasmalemma of *Samanea* motor cells, we tested its interaction with several different ions: the alkali series (Li^+ , Na^+ , Rb^+ and Cs^+), two divalent cations: Ba^{2+} and Cd^{2+} , and one trivalent member of the lanthanide group: Gd^{3+} . This characterization should aid in evaluating the role of this channel in the volume changes of intact protoplasts.

Selectivity to Monovalent Cations

The relative permeability of other monovalent ions (compared to that of K^+) in the K_D channel was calculated using

the Goldman equation (Eq. 1 in "Materials and Methods"). Rb^+ is the second most permeant ion, after K^+ , with permeability values ranging between 0.4 and 0.8. Na^+ , Cs^+ and Li^+ have small and comparable permeabilities, but they differ dramatically in that Li^+ and Na^+ have relatively little effect on K^+ currents (Figs. 1B and 4A), while Cs^+ blocks them (Figs. 3 and 4B).

Both the differences and the similarities in the permeabilities of the ions through the K_D channel can be explained in terms of the free energy profile for ion diffusion in this channel. Generally, the path of a permeating ion can be described as a spatial potential energy profile with maxima (barriers) and minima or wells (sites of interaction). The height of the energy barrier for an ion to enter the channel reflects the energy balance of substituting its hydration layers by solvation by the polar groups within the channel. The higher the barrier the less likely the ion will enter the channel. The higher the internal barriers or the tighter the interaction of an ion with a site within the channel, i.e. the deeper the well, the slower the permeation through the channel (3, 5, 13).

Thus, K^+ and Rb^+ enter the *Samanea* K_D channel with a

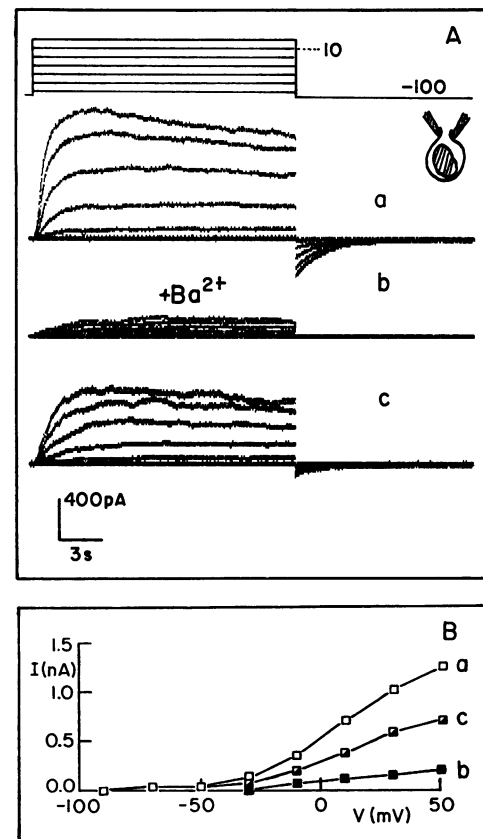


Figure 6. Reversibility of Ba^{2+} block. (A) Membrane currents (superimposed), in response to a series of square voltage pulses (also superimposed), before (a) and during (b) treatment with external Ba^{2+} (1 mM), and after washout to estimated final $[\text{Ba}^{2+}]$ of $<5 \mu\text{M}$ (c). During the wash potential was held at -100 mV . (B) Steady-state I - V curves corresponding to conditions in A. Solutions: as in Figure 1A.

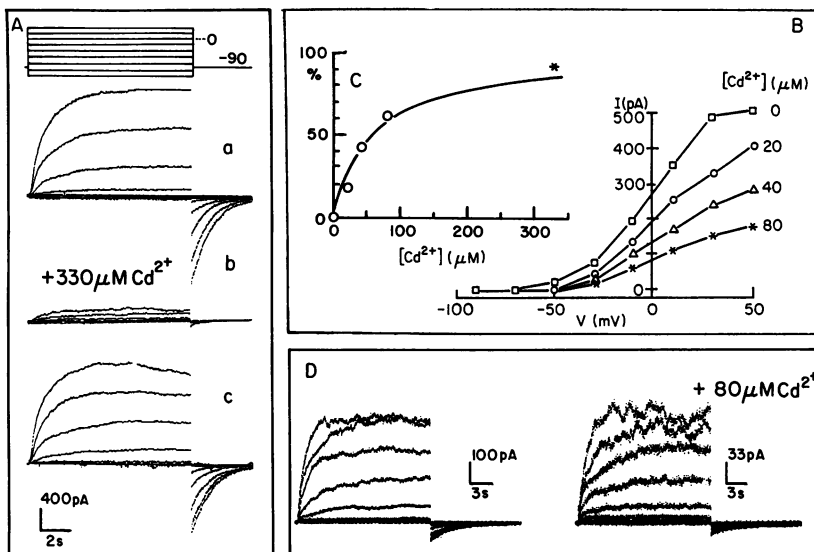


Figure 7. Effect of Cd^{2+} on K^+ currents. (A) Membrane currents (superimposed) in an extensor cell, in response to a series of square voltage pulses (also superimposed), before (a) and after (b) the addition of external Cd^{2+} ($330 \mu\text{M}$), and after washout (c) to estimated final $[\text{Cd}^{2+}]$ of $<10 \mu\text{M}$. Between pulses and during the wash, membrane potential was held at -90 mV . (B) Steady-state I - V curves from a flexor cell, from membrane currents obtained with various Cd^{2+} concentrations, indicated to the right. (C) Percentage of block by Cd^{2+} versus external $[\text{Cd}^{2+}]$, at $+50 \text{ mV}$ for data of B (circles) and at $+40 \text{ mV}$ for data of A (asterisk). Line: a least-mean-square fit to the experimental points (circles, not including the asterisk), of Michaelis-Menten-type equation: $I = 100/(1 + K_o/S)$; with I denoting percent inhibition of K^+ current, as compared to control; S , $[\text{Cd}^{2+}]$, and K_o , the dissociation constant for the binding of Cd^{2+} to its blocking site, $= 58 \pm 8 \mu\text{M}$. (D) Comparison between K^+ currents without (left) and with (right) $80 \mu\text{M}$ Cd^{2+} in the bath. Note the different vertical scales for the current. Solutions as in Figure 1A, except: A, bath: 55 mM K^+ , 52 mM Cl^- (pH 5.8); pipette: 214 mM K^+ , 200 mM Cl^- , 2 mM EGTA (instead of BAPTA), 1.96 mM Ca^+ (calculated free Ca^{2+} concentration: $3 \mu\text{M}$ [6]); B to D, as in Figure 1A.

relatively low energy barrier and cross the channel with relatively small interaction with a site(s) within. The low permeability of Li^+ and Na^+ may be due to a much higher energy barrier for entering the channel from outside. We did not test the effects of internal Li^+ and Na^+ (although some Na^+ was included in most of the internal solutions used), and thus have no information on the interaction of these ions with the internal mouth of the channel. In contrast, the low permeability of Cs^+ combined with its blocking of K^+ current may be ascribed to its much stronger interaction within the channel (see also below). In the sequence of relative permeability, the *Samanea* depolarization-activated K^+ channel resembles several other types of K^+ channels in membranes of animal cells (reviewed by Hille [14]) and in plant cells (25–27).

K_o Channel as a Long Pore: Cs^+ and Ba^{2+} Block

A complete block by Cs^+ occurs when the current flows away from the side of Cs^+ application (e.g. inward current with Cs^+ applied externally, Figure 4B, or, outward current with Cs^+ applied internally, Fig. 5A). However, the block is only partial when the current flows toward the Cs^+ side (outward currents in Fig. 4B, and tail-currents in Fig. 5A). Such directional, or voltage-dependent, block by Cs^+ has been observed in various types of K^+ channels in animal cell membranes (3, 8, 9, 12), and is consistent with a view that Cs^+ interacts strongly with a site(s) within the channel, resulting in its own very slow permeation and occlusion of the movement of K^+ (3). According to this view, K^+ entering the channel from the Cs^+ side would trap the Cs^+ inside and be itself prevented from crossing, while K^+ entering from the opposite side, would relieve the block by repelling Cs^+ off the site (2, 15). Such a mutual interaction of ions present simul-

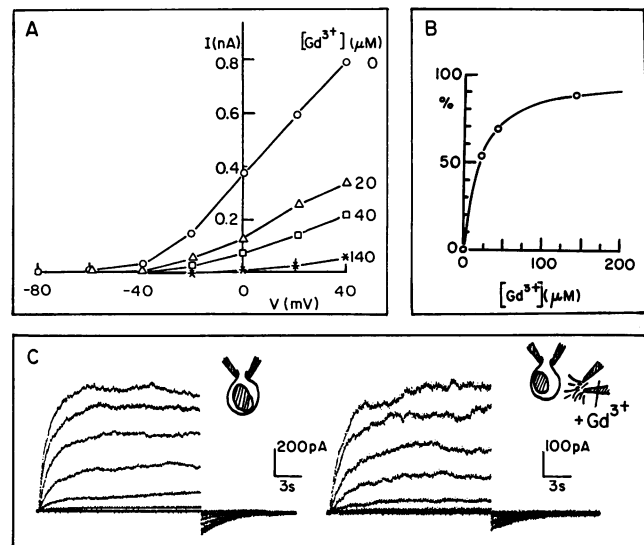


Figure 8. Effect of Gd^{3+} on K^+ currents. (A) Steady-state I - V curves from an extensor cell, from membrane currents obtained with various Gd^{3+} concentrations, indicated (in μM) to the right. (B) Percentage of block by Gd^{3+} versus external $[\text{Gd}^{3+}]$, at $+50 \text{ mV}$. Line: a least-mean-square fit of the Michaelis-Menten relation (as in Fig. 7 legend), to the experimental points, with $K_o = 17.4 \pm 0.3 \mu\text{M}$. (C) K^+ currents before (left) and during (right) exposure of the membrane to external solution containing 0.2 mM Gd^{3+} diffusing from a nearby pipette (inset). Note the difference in vertical scales for the currents. Solutions as in Figure 1A.

taneously within the channel led to the concept of a 'long pore.' Thus, as suggested by the Cs⁺ block of K⁺ permeation, the *Samanea* K_D channel is similar to 'long-pore' K⁺ channels in other systems.

Similarly to Cs⁺, Ba²⁺ has been shown to block K⁺ passage through several types of K⁺ channels in animal cell membranes by occlusion of the open channel (1, 4, 16, 29). In the Ca²⁺-dependent K⁺ channel, the block is voltage dependent, as though Ba²⁺ bound at a site located about 80% of the length of the channel, from the inside (assuming a linear voltage drop across the channel). The binding of Ba²⁺ is competitive with K⁺, and block by Ba²⁺ can be relieved by K⁺ (20, 29).

Since the occupancy of the site by Ba²⁺ stabilizes the K⁺ channel in the open conformation (albeit, most of it in the nonconducting, occluded state), and since Ba²⁺ becomes trapped in the closed channel (16), the gating kinetics of the channel is expected to slow down, and holding the membrane at a hyperpolarized potential (which favors the closed state of the channel) should slow down the washout of Ba²⁺ effect. Indeed, in the *Samanea* K_D channel, we observed (a) an increase of *t*_{1/2} for channel activation when the external solution contained Ba²⁺ (Fig. 5A) and (b) much slower washout of Ba²⁺, as compared to that of other ions (Fig. 6).

In the *Samanea* K_D channel, external Ba²⁺ blocks inward K⁺ currents much more strongly than it blocks outward K⁺ currents (Fig. 5, A and B). This voltage dependence of the block is consistent with the Ba²⁺ block occurring within the K_D channel. The dependence of the amount of block by external Ba²⁺ on the concentration of external K⁺ is consistent with the two ions interacting at a common site within the channel, as in the K⁺ channels in the animal cell membranes (16, 20, 29). This interaction is also consistent with the long-pore view of the K_D channel.

An important practical consequence from the "long pore" behavior of the *Samanea* K_D channel is that the relative permeabilities of various ions in this channel may vary, depending on the concentrations of the ions near the channel ("anomalous mole fraction effect"; reviewed by Hille [14]), as shown recently for K⁺ channels in *Chara* by Tester (28). This, most probably, is the reason for the relatively large range of permeability values obtained in our experiments, and should be a reason for caution in comparing data obtained in different experimental situations.

Cd²⁺ and Gd³⁺ Block; A Direct or Indirect Interaction with K_D Channel?

Cadmium block of the K⁺ channel seems to lack the properties of the Ba²⁺ block, that characterize an interaction *within* the channel. Cd²⁺ block seems to be independent of voltage (Fig. 7B), and of the external K⁺ concentration (Fig. 7, B and C), and the kinetics of the currents seem unaffected by Cd²⁺ (Fig. 7D).

Cd²⁺ may block the K_D channel directly (although not within its lumen); alternatively, the mechanism for K⁺ current inhibition by Cd²⁺, could be indirect, via the blockade of Ca²⁺ channels. This requires an additional assumption, that the K⁺ channel opening is Ca²⁺ dependent, and that it is activated due to Ca²⁺ influx through Ca²⁺ channels that open upon

depolarization. Ca²⁺ dependence has not yet been demonstrated for the *Samanea* K_D channel. Moreover, in experiments with internal free Ca²⁺ buffered to about 40 nM (with either EGTA or BAPTA), K⁺ currents were not appreciably different from those recorded with internal free Ca²⁺ of about 3 μM. This apparent insensitivity to internal Ca²⁺ concentration renders it rather unlikely that the channel is Ca²⁺-dependent. However, since in all our experiments the external Ca²⁺ concentration was 1 mM, we cannot rule out a transient local increase in internal Ca²⁺ concentration, if depolarization activated putative Ca²⁺ channels. Interestingly, we have observed Ca²⁺-permeable channels in the plasmalemma of extensors cell protoplasts (19). If these are juxtaposed to the K⁺ channels in the membrane, the local rise in internal Ca²⁺ might be sufficient to activate the K⁺ channel. In this case, the effect of Cd²⁺ on the *Samanea* K_D channel would be consistent with its well known blocking effect of the Ca²⁺ channel in animal cells (reviewed by Hille [14]).

Gd³⁺ appears to block the K_D channel in a similar fashion. In lieu of evidence that Gd³⁺ blocks the K_D channel directly, we suggest that its effect may be exerted indirectly, as proposed for Cd²⁺. La³⁺, an ion similar to Gd³⁺, has been shown to block Ca²⁺ channels in several animal preparations (10).

Thus, the blocking effect of Cd²⁺ and Gd³⁺ on *Samanea* K⁺ currents provides incentive for further investigation of the Ca²⁺-permeable channels in pulvinar motor cells, on one hand, and of extending the search for Ca²⁺ effect on the K_D channel, on the other hand.

ACKNOWLEDGMENTS

We thank Dr. M. J. Morse and G. Y. Yueh for help in modifying our protoplast isolation technique, and Dr. M. Segal for continuous encouragement, support, and valuable discussions.

LITERATURE CITED

1. **Armstrong CM, Taylor SR** (1989) Interaction of barium ions with potassium channels in squid giant axons. *Biophys J* **30**: 473-488
2. **Armstrong CM, Binstock L** (1965) Anomalous rectification in the squid giant axon injected with tetraethylammonium chloride. *J Gen Physiol* **48**: 859-872
3. **Bezanilla F, Armstrong CM** (1972) Negative conductance caused by entry of sodium and cesium ions into the potassium channels of squid axons. *J Gen Physiol* **60**: 588-608
4. **Eaton DC, Brodwick MS** (1980) Effect of barium on the potassium conductance of squid axons. *J Gen Physiol* **75**: 727-750
5. **Eisenman G, Horn R** (1983) Ionic selectivity revisited: the role of kinetic and equilibrium processes in ion permeation through channels. *J Membr Biol* **76**: 197-225
6. **Fabiato A, Fabiato G** (1979) Calculations for computing the compositions of the solutions containing multiple metals and ligands used for experiments in skinned muscle cells. *J Physiol (Paris)* **75**: 463-505
7. **Goldman DE** (1943) Potential, impedance and rectification in membranes. *J Gen Physiol* **27**: 37-60
8. **Gorman ALF, Woolum JC, Cornwall MC** (1982) Selectivity of the Ca²⁺-activated and light-dependent K⁺ channels for monovalent cations. *Biophys J* **38**: 319-322
9. **Hagiwara S, Takahashi K** (1974) The anomalous rectification and cation selectivity of the membrane of a starfish egg cell. *J Membr Biol* **18**: 61-80
10. **Hagiwara S, Takahashi K** (1967) Surface density of calcium ions and calcium spikes in the barnacle muscle fiber membrane. *J Gen Physiol* **50**: 583-601

11. **Hamil OP, Marty A, Neher E, Sakmann B, Sigworth FJ** (1981) Improved patch-clamp techniques for high resolution current recording from cells and cell-free membrane patches. *Pflugers Arch* **391**: 85–100
12. **Hille B** (1973) Potassium channels in myelinated nerve. Selective permeability to small cations. *J Gen Physiol* **61**: 669–687
13. **Hille B** (1975) Ionic selectivity of Na and K channels of nerve membranes. In G Eisenman, ed, *Membranes—A Series of Advances*, 3. Lipid Bilayers and Biological Membranes: Dynamic Properties. Marcel Dekker, New York, pp 255–323
14. **Hille B** (1984) *Ionic Channels of Excitable Membranes*. Sinauer Associates, Sunderland, MA
15. **Hille B, Schwarz W** (1978) Potassium channels as multi-ion single-file pores. *J Gen Physiol* **72**: 409–442
16. **Miller C, Latorre R, Reisin I** (1987) Coupling of voltage-dependent gating and Ba^{2+} block in the high-conductance, Ca^{2+} -activated K^+ channel. *J Gen Physiol* **90**: 427–449
17. **Moran N, Ehrenstein G, Iwasa K, Mischke C, Bare C and Satter RL** (1988) Potassium channels in motor cells of *Samanea saman*: a patch-clamp study. *Plant Physiol* **88**: 643–648
18. **Moran N, Satter RL** (1988) Inorganic ions and K^+ channels in *Samanea* protoplasts (abstract No. 780). *Plant Physiol* **86**: S-130
19. **Moran N, Satter RL** (1989) Depolarization-activated inward currents in motor cells of *Samanea saman* (abstract No. 269). *Plant Physiol* **89**: S-45
20. **Neyton J, Miller C** (1988) Discrete Ba^{2+} block as a probe of ion occupancy and pore structure in the high-conductance Ca^{2+} -activated K^+ channel. *J Gen Physiol* **92**: 569–586
21. **Robinson RA, Stokes RH** (1965) *Electrolyte Solutions*. Butterworths, London
22. **Satter RL, Galston AW** (1981) Mechanisms of control of leaf movements *Annu Rev Plant Physiol* **32**: 83–110
23. **Satter RL, Moran N** (1988) Ionic channels in plant cell membranes. *Physiol Plant* **72**: 816–820
24. **Satter RL, Morse MJ, Lee Y, Crain RC, Cote G, Moran N** (1988) Light- and clock-controlled leaflet movements in *Samanea saman*: a physiological, biophysical and biochemical analysis. *Bot Acta* **101**: 205–213
25. **Schroeder JI, Rashke K, Neher E** (1987) Voltage dependence of K^+ channels in guard cell protoplasts. *Proc Natl Acad Sci USA* **84**: 4108–4112
26. **Schroeder JI** (1988) K^+ transport properties of K^+ channels in the plasma membrane of *Vicia faba* guard cells. *J Gen Physiol* **92**: 667–683
27. **Tester M** (1988) Blockade of potassium channels in the plasmalemma of *Chara corallina* by tetraethylammonium, Ba^{2+} , Na^+ and Cs^+ . *J Membr Biol* **105**: 77–85
28. **Tester M** (1988) Potassium channels in the plasmalemma of *Chara corallina* are multi-ion pores: voltage-dependent blockade by Cs^+ and anomalous permeabilities. *J Membr Biol* **105**: 87–94
29. **Vergara CE, Latorre R** (1983) Kinetics of Ca^{2+} -activated K^+ channels from rabbit muscle incorporated into planar bilayers. Evidence for a Ca^{2+} and Ba^{2+} blockade. *J Gen Physiol* **82**: 543–568